

# Supporting Information:

## Structuring Gelatin Methacryloyl - Dextran Hydrogels and Microgels Under Shear

Ghazi Ben Messaoud,<sup>\*,†,‡</sup> Evdokia Stefanopoulou,<sup>†</sup> Mattis Wachendörfer,<sup>¶</sup> Sanja  
Aveic,<sup>¶</sup> Horst Fischer,<sup>¶</sup> and Walter Richtering<sup>\*,§,‡</sup>

<sup>†</sup>*Institute of Physical Chemistry, RWTH Aachen University, Landoltweg 2, 52074 Aachen,  
Germany, European Union*

<sup>‡</sup>*DWI-Leibniz Institute for Interactive Materials, Forckenbeckstrasse 50, 52074  
Aachen, Germany, European Union*

<sup>¶</sup>*Department of Dental Materials and Biomaterials Research, RWTH Aachen University  
Hospital, 52074 Aachen, Germany*

<sup>§</sup>*Institute of Physical Chemistry, RWTH Aachen University, Landoltweg 2, 52074  
Aachen, Germany, European Union*

E-mail: benmessaoud@dwil.rwth-aachen.de; richtering@rwth-aachen.de

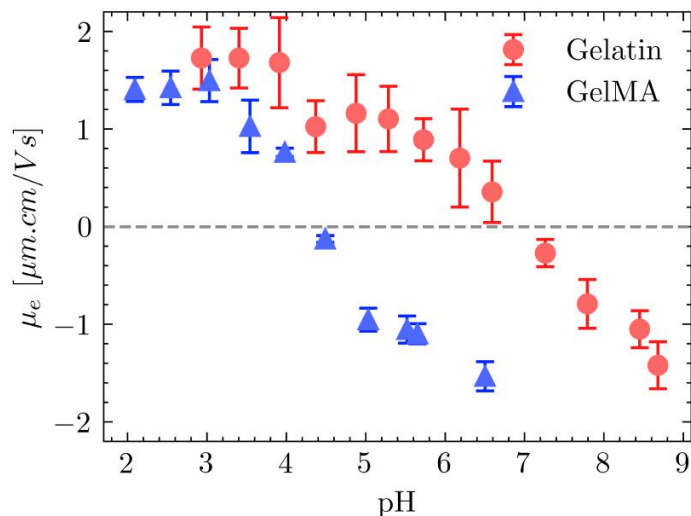


Figure S1: Evolution of the electrophoretic mobility ( $\mu_e$ ) of native gelatin and GelMA as a function of pH

## Shear viscosity of GelMA-dextran ATPS

Shear viscosity as a function of the shear rate ( $\dot{\gamma}$ ) of GelMA, dextran solutions and their mixtures, and their phase-separated fractions were measured at 37°C using a DHR3 rheometer equipped with a cone plate geometry (40 mm, 1.986 ° and a truncation of 57  $\mu\text{m}$ ). Regarding GelMA-dextran mixtures, the influence of the time of the shear rate ramp was investigated based on the previous study by Tea et al.,<sup>S1</sup> Briefly, after sample loading in the rheometer, a preshear was applied at  $\dot{\gamma} = 10^3 \text{ s}^{-1}$  during 30 s followed by a descending shear rate ramp from  $10^3 \text{ s}^{-1}$  to  $10^{-2} \text{ s}^{-1}$  followed by an ascending shear rate ramp from  $10^{-2}$  to  $10^3 \text{ s}^{-1}$ . The influence of the duration of the shear rate ramp was investigated by varying the shear rate ramp time from 2 to 20 min.

The flow properties of GelMA/ Dextran mixtures were studied as a function of the shear rate ramp time, demonstrating that increasing the shear rate ramp time results in an increase of the viscosity at low shear rates and a decrease of the infinite shear viscosity Figure S2A-C.

An increase of HCl molarity from 14 mM to 18.5 mM, and therefore a decrease of the pH from pH 4.38 to pH 4.13, near the isoelectric point, results in a fast increase of the low shear viscosity as a function of the time of the shear rate ramp as highlighted by the evolution of the low shear viscosity as a function of the shear ramp time Figure S2D. This could indicate that the phase separation kinetics depend on the pH of the mixture as demonstrated previously.<sup>S2</sup> This is also in good agreement with the recent study on the gelatin-dextran mixture that demonstrates the pH-responsive phase separation kinetic and which could be related to the self-aggregation of gelatin as a function of the pH.<sup>S3</sup> In order to obtain comparable viscosity data, we selected a shear rate ramp time of 2 minutes Figure S3. An attempt to fit the shear viscosity data to models that were previously applied to describe the shear viscosity of water-in-water emulsion<sup>S1</sup> such as Frankel and Crevoris<sup>S4</sup> or the Kroy<sup>S5</sup> model was not successful. This is probably related to the low viscosity of the GelMA-dextran mixture.

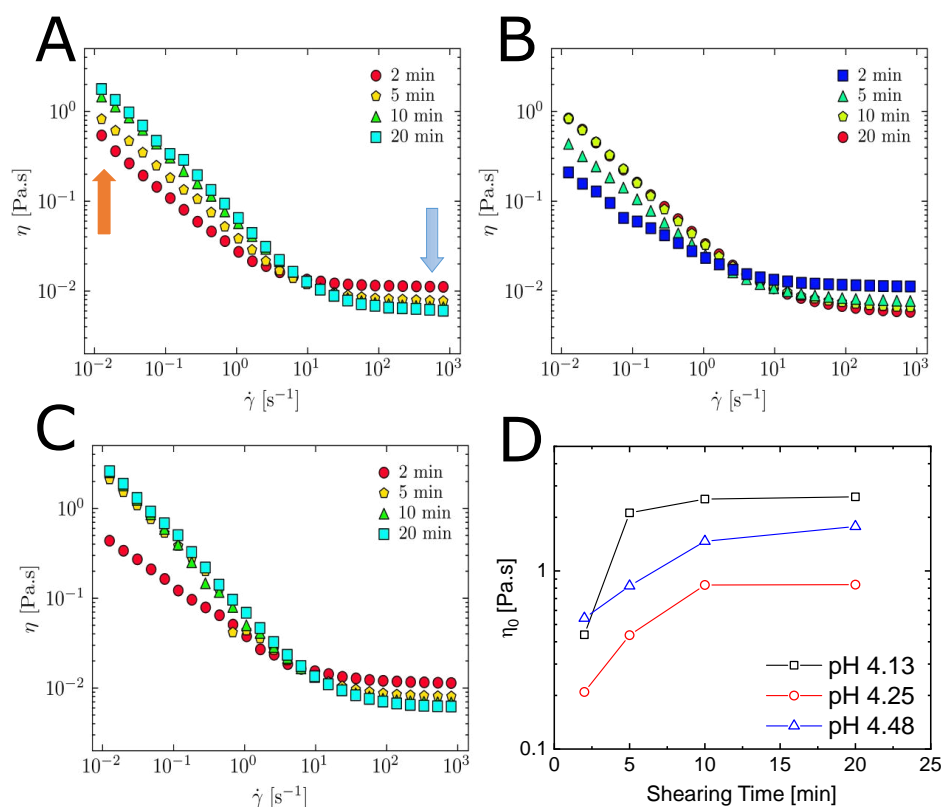


Figure S2: Influence of the time of the shear rate ramp on the shear viscosity evolution as a function of the shear rate for a D/G droplets system at A) pH 4.13, B) pH 4.25 and C) pH 4.38, D) evolution of the low shear viscosity as a function of the shear rate ramp.

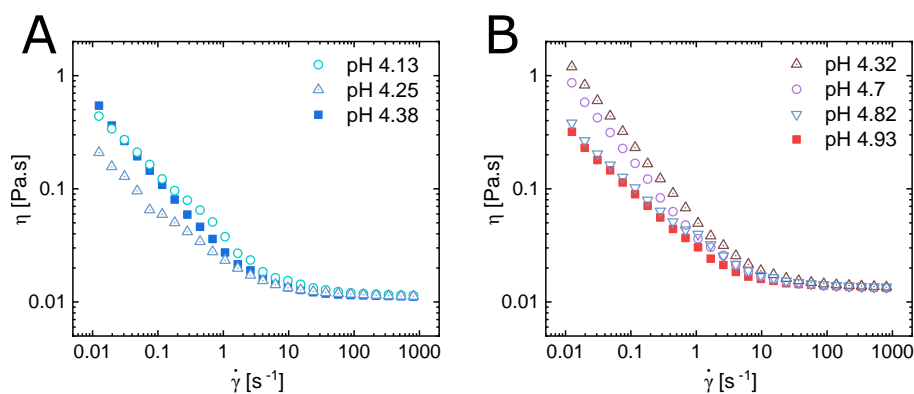


Figure S3: Evolution of the shear viscosity as a function of the shear rate ( $\dot{\gamma}$ ) for A) D/G droplets and the B) bicontinuous system as a function of pH.

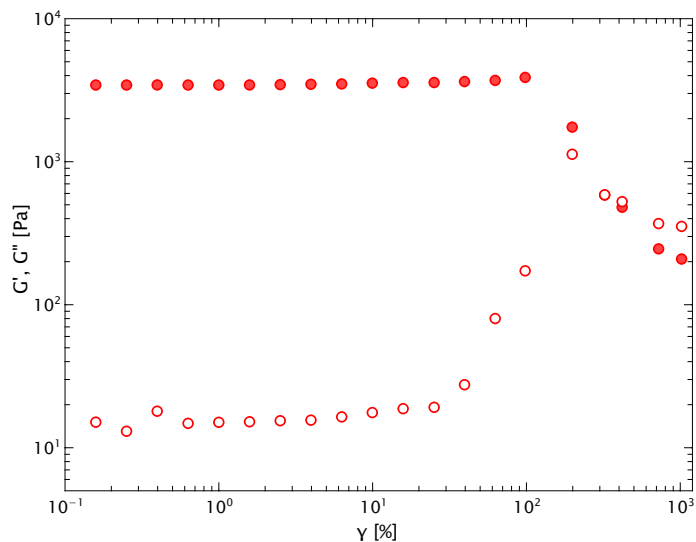


Figure S4: Evolution of the storage ( $G'$ ) and loss ( $G''$ ) moduli of GelMA hydrogel as a function of strain( $\gamma$ ) at  $f = 1 \text{ Hz}$  and room temperature

## Influence of the applied UV intensity on the gelation of GelMA

In the current work, we used Irgacure D2959, a widely used photoinitiator for the preparation of biomaterials such as GelMA hydrogels.<sup>S6</sup> It is a type I photoinitiator where photofragmentation generates radical pairs through a  $\alpha$ -cleavage process.<sup>S7</sup> During UV illumination, the absorption of UV photons leads to a conversion of the excited singlet state to a triplet state through intersystem crossing, and this triplet state dissociates to form benzoyl and ketyl radicals.<sup>S8</sup> The ketyl radical is short-lived since it rapidly reacts with water, and thus the benzoyl radical is the major initiating species.<sup>S7</sup>

To ensure a fast gelation kinetic of the GelMA-rich phase, the influence of the applied UV intensity on GelMA 52.8 mg/mL solution on the gelation kinetics was investigated by varying the UV intensity from 5 to 100  $mW/cm^2$  with a total illumination time of 4 minutes. A delay time between the start of illumination and the increase in the storage modulus ( $G'$ ) is observed(Figure S5). The delay time depends on the UV intensity applied and is 61.6, 37.2, 6.8, and 0.9 s for, respectively, the applied UV intensity of 5, 10, 50, and 100  $mW/cm^2$ . The delay time is generally related to inhibition of photocrosslinking by oxygen dissolved in the solution, which is a general phenomenon that affects free radical polymerization reactions.<sup>S9</sup> The observed delay times as a function of UV intensity are in good agreement with a previous study.<sup>S10</sup>

As mentioned, for a UV intensity of 100  $mW/cm^2$ , the delay time of photocrosslinking is  $d_t < 1 \text{ s}$ , and the second acquired data, after 6 s, show a  $G' \sim 100 \text{ Pa}$ , which is typical of a solid-like behavior. Complete gelation, marked by  $G'$  reaching a plateau, is achieved after 60 s of illumination. On the basis of this observation, a UV intensity of 100  $mW/cm^2$  was selected for the UV-rheology study. The UV exposure time is decreased from 240 s to 120 s to avoid potential dye degradation, which eventually alters the quality of subsequent CLSM imaging.

The influence of shear on the resulting hydrogel microstructure was therefore investi-

gated by applying a constant shear rate or shear stress for 60 s, followed by immediate UV photocrosslinking at  $100 \text{ mW/cm}^2$  for 120 s and the evolution of  $G'$  and  $G''$  as a function of time were monitored during 240 or 540 s. Afterward, a frequency sweep was conducted, and finally, the hydrogel microstructure was analyzed using CLSM. Figure S5A shows the evolution of  $G'$  as a function of time after applying UV and 60 seconds after starting the time-frequency sweep. All curves demonstrate an increase of the storage modulus after applying UV until reaching a plateau indicating the complete gelation of the system. The UV intensity does not appear to significantly affect the plateau storage modulus ( $G'_p$ ) of the hydrogels after complete gelation. Oxygen slows the onset of photocrosslinking either by quenching the excited triplet states of the photoinitiator or by reacting with the polymerizing radicals to generate peroxy radicals which are much less reactive towards double bonds<sup>S7,S10</sup> However, it was previously reported that replacing oxygen with nitrogen bubbling did not result in a significant decrease in the delay time in photorheology experiments since the required time to start the photorheology experiments ( $\approx 2\text{min}$ ) was sufficient to reequilibrate the oxygen level in solution<sup>S10</sup>

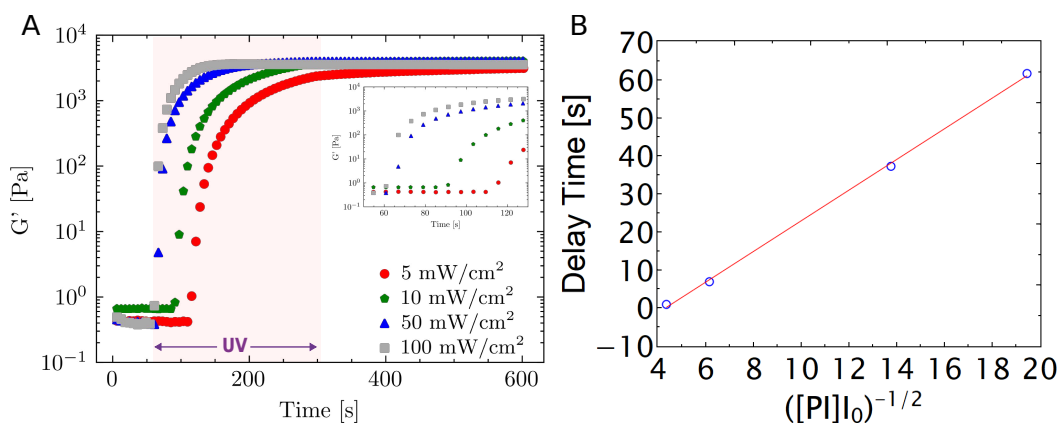


Figure S5: A) Influence of the applied UV intensity on the evolution of the storage modulus ( $G'$ ) during the gelation of GelMA 52.8 mg/mL solutions. UV illumination is applied during 240 s, and 60 s after the onset of the frequency-time sweep at  $f = 1 \text{ Hz}$  and  $\gamma = 5\%$ . The inset graph is a magnification of the data during the first 130 s to highlight the delay time between the onset of UV illumination and the increase of the ( $G'$ ), B) Linear relationship between the delay time and the inverse of the square root of the product of the applied UV intensity and the photoinitiator concentration  $[PI]$ .

In the current study, the samples were not degassed because the objective was to load the final mixture as fast as possible on the rheometer after preparation. Moreover, although it was possible to degas the stock solutions priorly, the preparation conditions of the final mixture, i.e. pipetting the different solutions and vortexing, will allow fast re-equilibration of the oxygen level. The delay time ( $d_t$ ) was plotted as a function of the inverse square root of the product of the photoinitiator concentration  $[PI]$  and the applied intensity ( $I_0$ ) with  $d_t \equiv ([PI]I_0)^{-1/2}$  and is shown in Figure S5B. The data was fitted to a linear function. Although fitting with an affine function provides the best fit (slope = 4.03, constant = 17.46, and adjusted R squared of = 0.998), a linear function from origin also provides a good fit (slope = 2.81, adjusted R squared of = 0.926) and is in good agreement with a previous

study, where a slope of 2.73 was obtained. These well-determined exponents could be related to the intensity ranges previously investigated or the intrinsic properties of GelMA, mainly its degree of methacrylation of 73 % and 75% in the former and current study, respectively. The UV-rheology experiments were conducted at room temperature between 22 and 25 ° C with preheated mixtures at 37 ° C. This is due to the exchange of the Peltier lower part by the UV accessory. However, we should mention that during the shear step that lasted 60 seconds, we did not observe any increase in viscosity during the constant shear. This indicate that the selected time and temperature allow to avoid any possible physical gelation of the GelMA phase through the structural transition from random coil to triple helix.<sup>S11</sup>

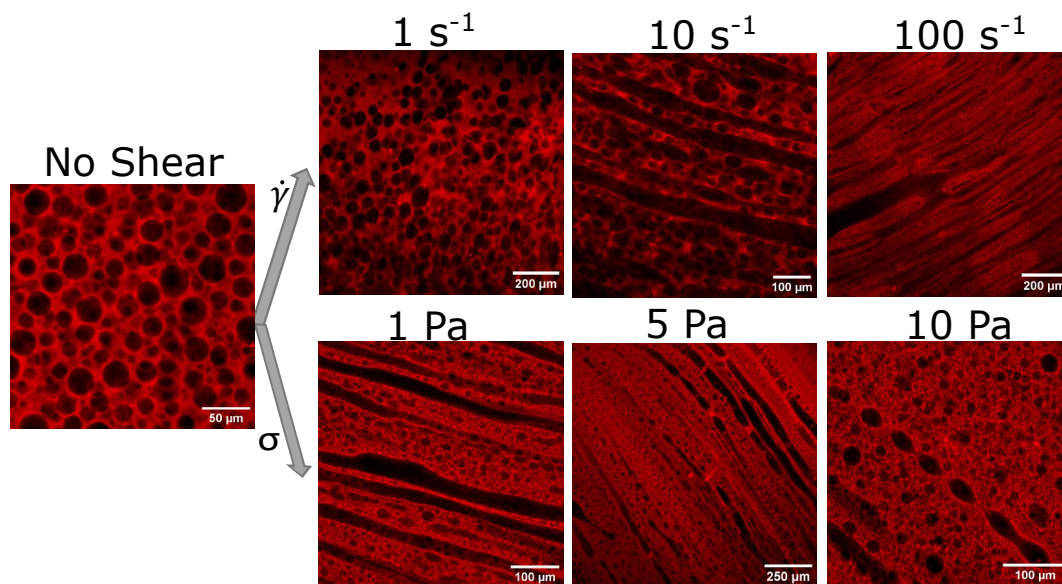


Figure S6: Additional CLSM images of the D/G system after applying a constant shear rate or shear stress during 60 seconds followed by photocrosslinking.



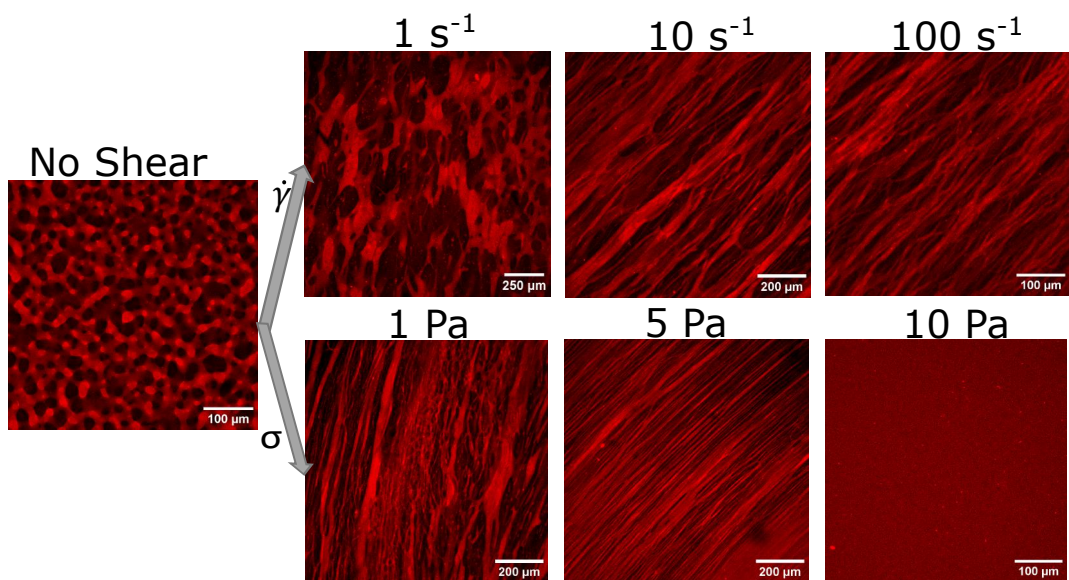


Figure S7: Additional CLSM images of the bicontinuous system after applying a constant shear rate or shear stress during 60 seconds followed by photocrosslinking.

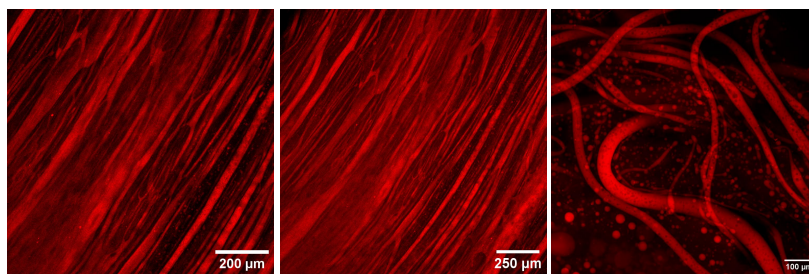


Figure S8: CLSM images of hydrogel resulting from a preshear of a bicontinuous system and consisting of an oscillatory shear strain of 50 % at a frequency  $f = 1$  Hz

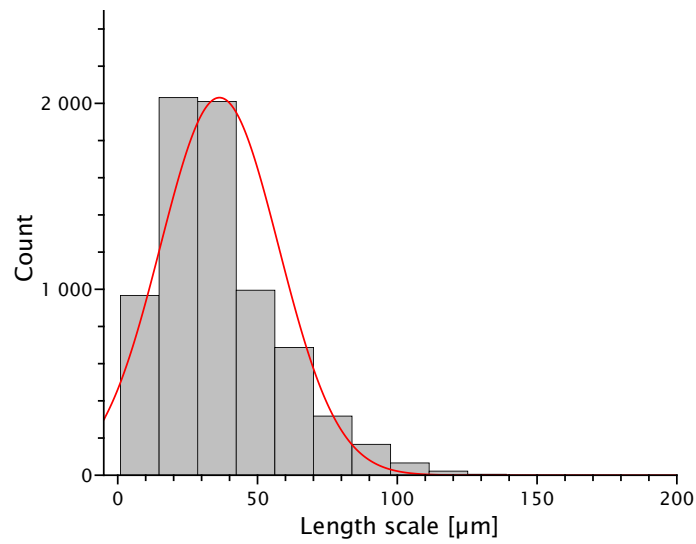


Figure S9: Characteristic length scale distribution of the bicontinuous system used for geometry confinement experiments.

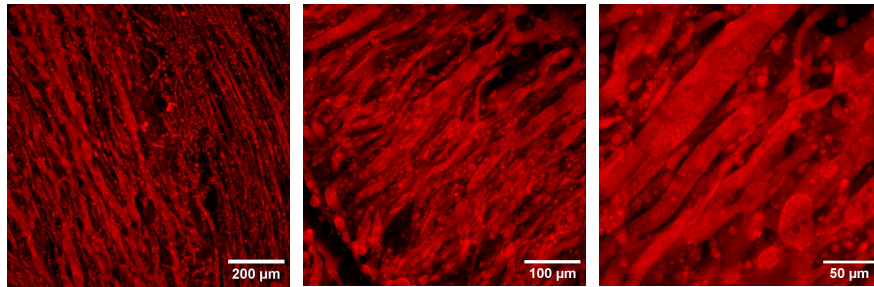


Figure S10: Additional CLSM image of the bicontinuous hydrogel prepared in the absence of a preshear and using a gap size of 50  $\mu m$ .

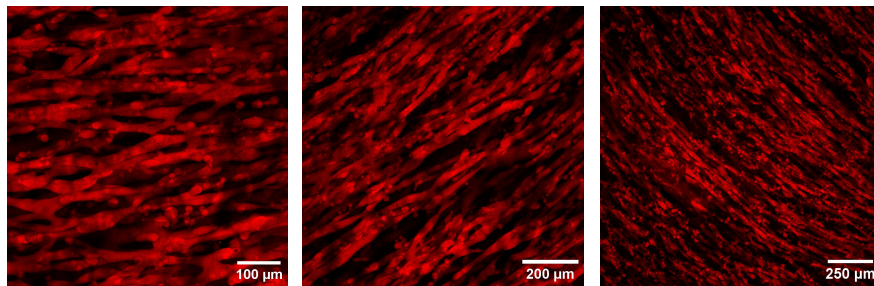


Figure S11: Additional CLSM images demonstrating the formation of microfilaments coexisting with GelMA clusters at pH 4.7.



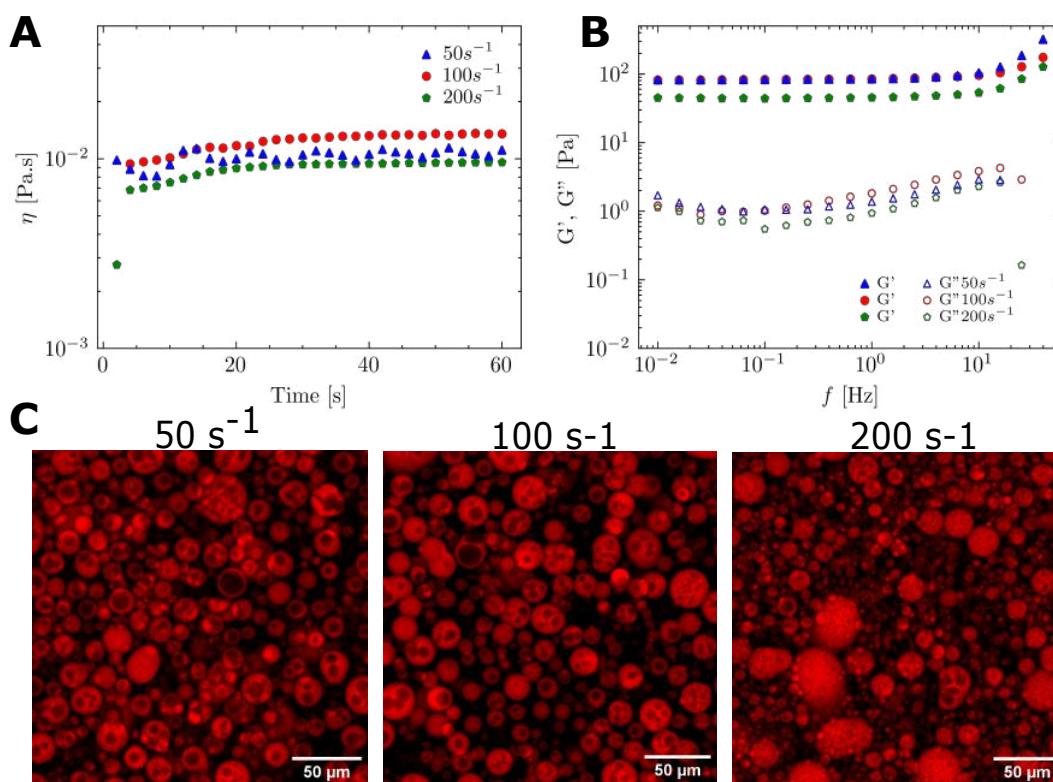


Figure S12: Influence of the shear rate on the macroporous GelMA microgels microstructure from a bicontinuous system at pH 4.6, A) viscosity evolution of the system during the preshear step, B) Frequency dependence of  $G'$  and  $G''$  and C) microstructure of the microgels resulting from a preshear rate of 50, 100 and 200  $s^{-1}$

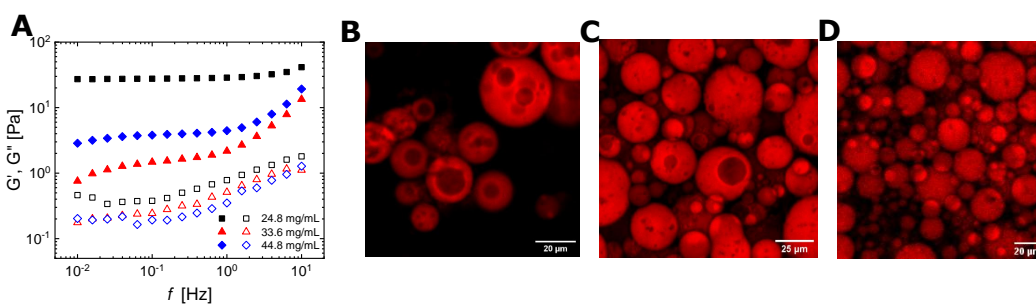


Figure S13: Influence of the shear rate on the macroporous GelMA microgels microstructure from bicontinuous system at pH 4.6, as a function of dextran concentration. A)  $G'$  and  $G''$  as a function of frequency, and CLSM images for dextran B) 24.8 mg/mL, C) 33.6 mg/mL and D) 44.8 mg/mL.

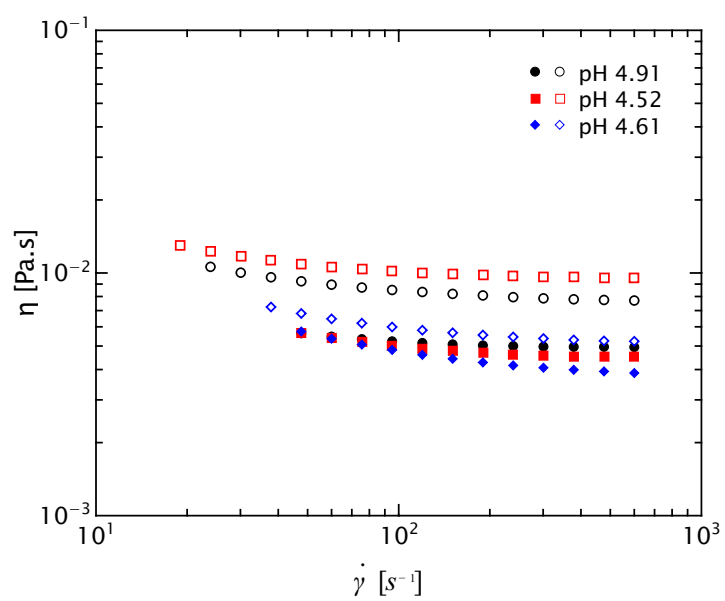


Figure S14: Shear viscosity as a function of shear rates for bicontinuous systems at pH 4.91 and pH 4.53 and D/G emulsion at a pH 4.61. The solid symbols represent the dextran-rich upper phase and the open symbols the GelMA-rich bottom phase.

## References

- (S1) Tea, L.; Nicolai, T.; Benyahia, L.; Renou, F. Viscosity and morphology of water-in-water emulsions: The effect of different biopolymer stabilizers. *Macromolecules* **2020**, *53*, 3914–3922.
- (S2) Ben Messaoud, G.; Aveic, S.; Wachendoerfer, M.; Fischer, H.; Richtering, W. 3D Printable Gelatin Methacryloyl (GelMA)-Dextran Aqueous Two-Phase System with Tunable Pores Structure and Size Enables Physiological Behavior of Embedded Cells In Vitro. *Small* **2023**, 2208089.
- (S3) Wang, Q.; Guo, Q.; Niu, W.; Wu, L.; Gong, W.; Yan, S.; Nishinari, K.; Zhao, M. The pH-responsive phase separation of type-A gelatin and dextran characterized with static multiple light scattering (S-MLS). *Food Hydrocolloids* **2022**, *127*, 107503.
- (S4) Frankel, N.; Acrivos, A. The constitutive equation for a dilute emulsion. *Journal of Fluid Mechanics* **1970**, *44*, 65–78.
- (S5) Kroy, K.; Capron, I.; Djabourov, M. On the Viscosity of Emulsions. *arXiv preprint physics/9911078* **1999**,
- (S6) Loessner, D.; Meinert, C.; Kaemmerer, E.; Martine, L. C.; Yue, K.; Levett, P. A.; Klein, T. J.; Melchels, F. P.; Khademhosseini, A.; Hutmacher, D. W. Functionalization, preparation and use of cell-laden gelatin methacryloyl-based hydrogels as modular tissue culture platforms. *Nature protocols* **2016**, *11*, 727–746.
- (S7) Andrzejewska, E. Photopolymerization kinetics of multifunctional monomers. *Progress in polymer science* **2001**, *26*, 605–665.
- (S8) Liu, M.; Li, M.-D.; Xue, J.; Phillips, D. L. Time-resolved spectroscopic and density functional theory study of the photochemistry of irgacure-2959 in an aqueous solution. *The Journal of Physical Chemistry A* **2014**, *118*, 8701–8707.
- (S9) Dendukuri, D.; Panda, P.; Haghgoie, R.; Kim, J. M.; Hatton, T. A.; Doyle, P. S. Modeling of oxygen-inhibited free radical photopolymerization in a PDMS microfluidic device. *Macromolecules* **2008**, *41*, 8547–8556.
- (S10) O’Connell, C. D.; Zhang, B.; Onofrillo, C.; Duchi, S.; Blanchard, R.; Quigley, A.; Bourke, J.; Gambhir, S.; Kapsa, R.; Di Bella, C., et al. Tailoring the mechanical properties of gelatin methacryloyl hydrogels through manipulation of the photocrosslinking conditions. *Soft matter* **2018**, *14*, 2142–2151.
- (S11) Van Den Bulcke, A. I.; Bogdanov, B.; De Rooze, N.; Schacht, E. H.; Cornelissen, M.; Berghmans, H. Structural and rheological properties of methacrylamide modified gelatin hydrogels. *Biomacromolecules* **2000**, *1*, 31–38.